Assessment of Elevation Uncertainty in Salt Marsh Environments using Discrete-Return and Full-Waveform Lidar

Authors: Rogers, Jeffrey N., Parrish, Christopher E., Ward, Larry G., and Burdick, David M.

Source: Journal of Coastal Research, 76(sp1) : 107-122

Published By: Coastal Education and Research Foundation

URL: https://doi.org/10.2112/SI76-010

Journal of Coastal Research	SI	76	107–122	Coconut Creek, Florida	2016

Assessment of Elevation Uncertainty in Salt Marsh Environments using Discrete-Return and Full-Waveform Lidar

Jeffrey N. Rogers[†‡*], Christopher E. Parrish[§Φ], Larry G. Ward[ϕ††], and David M. Burdick[ε††]

[†]Department of Earth Sciences
University of New Hampshire
Durham, NH 03824, U.S.A.

[‡]Center for Coastal Studies
Provincetown, MA 02657, U.S.A.

[§]School of Civil and Construction Engineering
Oregon State University
Corvallis, OR 97331, U.S.A.

[ϕ]Center for Coastal and Ocean Mapping/Joint Hydrographic Center
School of Marine Science and Ocean Engineering
University of New Hampshire
Durham, NH 03824, U.S.A.

[ε]Department of Natural Resources and the Environment
University of New Hampshire
Durham, NH 03824, U.S.A.

[††]Jackson Estuarine Laboratory
School of Marine Science and Ocean Engineering
University of New Hampshire
Durham, NH 03824, U.S.A.

www.cerf-jcr.org

www.JCRonline.org

ABSTRACT

Rogers, J.N.; Parrish, C.E.; Ward, L.G., and Burdick, D.M., 2016. Assessment of elevation uncertainty in salt marsh environments using discrete-return and full-waveform lidar. *In*: Brock, J.C.; Gesch, D.B.; Parrish, C.E.; Rogers, J.N., and Wright, C.W. (eds.), *Advances in Topobathymetric Mapping, Models, and Applications*. *Journal of Coastal Research*, Special Issue, No. 76, pp. 107–122. Coconut Creek (Florida), ISSN 0749-0208.

Lidar data can serve as an important source of elevation information for studying, monitoring and managing salt marshes. However, previous studies have shown that lidar data tend to have greater vertical uncertainty in salt marshes than in other environments, hindering the ability to resolve small elevation differences that can be ecologically significant in marshes. For coastal scientists and managers to effectively collect, evaluate, and/or use lidar data in salt marshes, factors affecting elevation uncertainty (*e.g.*, plant species, season, and lidar processing methods) must be well understood. This study addresses this need using discrete-return (DRL) and full-waveform lidar, along with field-surveyed reference data, for four marshes on Cape Cod, Massachusetts (USA). The lidar bias and standard deviation were computed across all four marsh systems and four major taxa using varying interpolation and filtering methods. The effects of seasonality were also investigated using lidar data acquired in the summer and the following spring. Relative uncertainty surfaces (RUS) were computed from lidar waveform-derived metrics and examined for their utility and correlation with individual lidar errors. The results clearly illustrate the importance of seasonality, species, and lidar interpolation and filtering methods on elevation uncertainty in salt marshes. Results also demonstrate that RUS generated from lidar waveform features are useful in qualitative assessments of lidar elevation uncertainty and correlate well with vegetation height (r = 0.85; n = 268). Knowledge of where DRL uncertainty persists within salt marshes and the factors influencing the higher uncertainty should facilitate the development of better correction methods.

ADDITIONAL INDEX WORDS: *Salt marsh vegetation, uncertainty,* Spartina alterniflora*, interpolation, bare earth filtering, inverse distance weighting, DEM*.

INTRODUCTION

Salt marshes are tidally influenced, halophytic grasslands found in middle and high latitudes around the globe (Mitsch and Gosselink, 2000). They are among the most productive ecosystems on the planet and provide valuable services to both the natural and human built environments, such as fish nursery habitat, carbon storage, sediment traps, water filtration, and shoreline protection (Costanza *et al*., 1997; Mitsch and Gosselink, 2000). The response of salt marshes to rising sea levels can be determined by very small variations in elevation, which affects inundation, available nutrients, sedimentation, and salinity (Morris *et al*., 2002). To monitor their health and response to changes in sea level rise (SLR), detailed topographic information on the order of centimeters is necessary. However, acquiring accurate terrain elevation data can be difficult and is typically costly and time-consuming if traditional data collection methods are used (Green, Carswell, and Gutelius, 1996). Lidar has been identified as a valuable tool for rapid survey of storm impacts, monitoring shoreline change, restoration planning, and flood hazard assessment (Brock and Sallenger, 2001) and is often proposed as a substitute for field-based datasets collected via differential leveling, trigonometric leveling with total stations, or Global Navigation Satellite System (GNSS) surveys (Montane and Torres, 2006; Schmid, Hadley, and Wijekoon, 2011).

Lidar's usefulness in salt marsh studies is a function of the uncertainty of lidar-derived elevation relative to the elevation range of ecological importance (Sadro, Gastil-Buhl, and Melack, 2007). For example, lidar in a salt marsh environment is

DOI: 10.2112/SI76-010 received 20 January 2015; accepted in revision 5 August 2015.
*Corresponding author: jrogers@coastalstudies.org

ineffective where its elevation uncertainty (due to vegetative variation and other factors) is greater than the elevation range determining inundation, species dominance, and habitat. In addition to impacts from vegetation, factors known to degrade the laser coordinates of points by centimeters to decimeters include sensor position and orientation (*i.e.*, the post-processed navigation solution from the GNSS-aided inertial navigation system (INS)), scan angle, calibration, and environmental parameters such as soil saturation (Hodgson and Bresnahan, 2004; Hopkinson *et al*., 2004; Lefsky *et al*., 2002; Shrestha and Carter, 1998). Based on all of these factors, especially the vegetation and environmental parameters, uncorrected lidar datasets generally have relatively high vertical uncertainty in salt marsh environments. Therefore, the lidar elevation datasets may be inadequate to determine inundation extent and frequency (Hladik and Alber, 2012; Morris *et al*., 2005; Rosso, Ustin, and Hastings, 2006; Schmid, Hadley, and Wijekoon, 2011), key factors influencing salt marsh health.

Research to determine the extent to which lidar achieves salt marsh canopy penetration has started to shed light on vegetation effects (Gopfert and Heipke, 2006; Hladik and Alber, 2012; Hladik, Schalles, and Alber, 2013; Populus *et al*., 2001; Rogers *et al*., 2015; Rosso, Ustin, and Hastings, 2006; Schmid, Hadley, and Wijekoon, 2011). Species stem density, vertical density, height, and seasonality likely influence lidar signal penetration properties in salt marsh environments. In addition to the physical attributes of vegetation height, leaf morphology and growth habit may also be factors influencing lidar signal returns (Hladik and Alber, 2012; Rogers *et al*., 2015). Leaf structures and growth habit vary greatly from species to species. For example, *Spartina alterniflora* has long flat tapering leaves and grows to a height of up to 2.0 m, while *Spartina patens* has narrow linear leaves that are rolled within a low growing ~0.1–0.3-m thatch in a "cow lick" pattern (Tiner, 1987). All of these vegetation attributes are likely to contribute to lidar error, while leading to point clouds that are difficult to distinguish visually from bare earth surfaces.

Notwithstanding the contributions of previous research, there is a need to better understand the factors affecting the vertical uncertainty of lidar data in salt marshes, such that coastal scientists and managers can make informed decisions related to a) assessment of when and how to use lidar data in salt marsh research, b) restoration planning, and c) sea level rise studies. This study addresses this need, using lidar data and RTK GNSS ground truth, for four salt marshes on Cape Cod, Massachusetts. Variables investigated include season (specifically, temporal differences between peak growth and senescent conditions), vegetation species, and lidar processing (interpolation and filtering) method.

Another important aspect of this study is the use of full-waveform lidar, which records a time series of backscattered signal strength for each laser pulse. Discrete-return lidar systems tend not to work well for mapping salt marshes for two reasons. First, discrete-return systems typically have a significant "dead zone" following each detected return (Nayegandhi *et al*., 2006). Due to this dead zone, a consecutive return typically cannot be detected for a surface 1.2–3.0 m below the first detected surface. Second, marsh vegetation is typically dense enough that the first return will almost always be from the top or somewhere near the top of the canopy, rather than the ground. The combination of these two factors makes it extremely challenging to perform bare earth elevation mapping of salt marshes with discrete-return lidar. By providing a time series of digitized return signal amplitude (rather than just discrete, detected returns), full-waveform systems can potentially provide greatly enhaced information in this challenging environment.

Techniques for working with full-waveform that are discussed in the literature typically involve sophisticated, computationally complex signal processing approaches such as deconvolution or decomposition into linear combinations of Gaussians (Jutzi and Stilla, 2006; Mallet and Bretar, 2009). Only a few studies have been conducted on the use of simple shape-based waveform metrics, such as width, numerical integral, slopes, skewness, and kurtosis (Adams, Beets, and Parrish, 2012; Collin *et al.*, 2011; Muss *et al*., 2013; Parrish, Rogers, and Calder, 2014; Rogers *et al.*, 2015). For purposes of this study, simple, shape-based waveform metrics are defined as features that contain information about the shape of the return waveform and that are computationally efficient to generate, with computation times typically being on the order of a few microseconds or less per laser pulse (Parrish, Rogers, and Calder, 2014). In this study, these features are used to create relative uncertainty surfaces (RUS) and assess spatial variation in elevation uncertainty throughout the marsh. These spatial assessments of uncertainty assist in answering the following types of questions: 1) where within the marsh are the elevations most reliable or suspect; 2) do the areas of high (or low) uncertainty overlap areas of particular concern, such as species transitions or critical habitat; and 3) if resources were available to support acquisition of

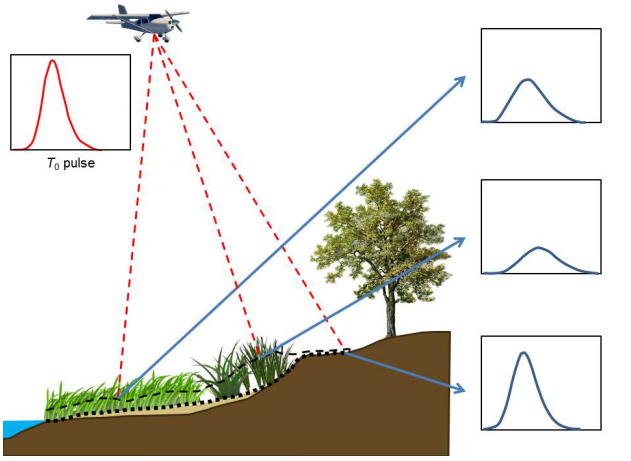

Figure 1: Lidar flight over a salt marsh. The black dotted line is ground measured with a RTK GNSS. The black dashed line is discrete lidar data returns of "ground." Also shown is the transmitted lidar pulse, T0, and the single pulse full-waveform returns based on the intercepted terrain and cover for three selected locations (arrows). Note: although the scene depicted in the figure is a cartoon representation of a marsh, the waveforms shown are real and were selected as representative of low marsh, high marsh, and bare earth. In all waveform plots, the y-axis is amplitude in arbitrary DNs, and the x-axis is discrete time index.

GNSS reference data within only a portion of the marsh, where should these efforts best be concentrated to achieve the greatest improvement in the marsh elevation data? Combined with the quantitative analysis of the DRL data, this information can assist coastal managers and scientists in more effectively utilizing lidar data of salt marshes.

METHODS

Four separate mesotidal salt marshes on protected coasts of Cape Cod, Massachusetts, USA, were investigated. The marsh sites chosen contained representative stands of the dominant plant species for the area (*Spartina alterniflora* Loisel*, Spartina patens, Distichlis spicata*, and *Salicornia spp.)* and were in close proximity of the marshes to each other, allowing field data to be collected within a specified time window around a lidar overflight. The sites from north to south are Hatches Harbor marsh (1.2 km^2), Moors marsh (2.0 km^2), Pamet marsh (2.0 km^2), and Great Island – Middle marsh (0.3 km^2) (Figure 2). The area has a semidiurnal tide with a mean range of ~2.83 m (NOAA, 2013). All the marshes surveyed in this study are low marsh environments with a sandy substrate and dominated by *Spartina alterniflora* (smooth cordgrass). Typically, there is a small border of high marsh located at the upland border dominated by *Spartina patens* (salt marsh hay), *Distichlis spicata,* and *Salicornia spp.* (glasswort) (Portnoy *et al*., 2003) (Figure 3). At two of the sites, Pamet River and Great Island, a large segment of the marsh appears to be in collapse, exhibiting extensive areas of bare ground due to a form of marsh wasting (Smith, 2009).

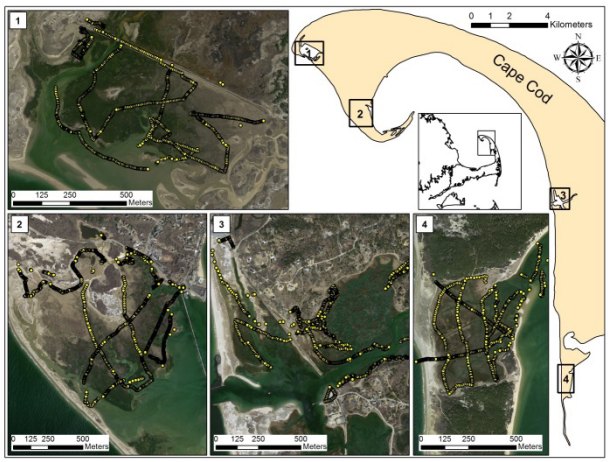

Figure 2: Site locus map and RTK GNSS points. Insets are 1) Hatches Harbor, 2) Moors marsh, 3) Pamet marsh, and 4) Great Island – Middle marsh.

The salt marsh vegetation in the study sites was characterized by homogeneous, near monoculture stands for three major species and one genus (*Spartina alterniflora, Spartina patens, Distichlis spicata*, and *Salicornia spp.)*. The vegetation demonstrated zonation patterns which are driven by small-scale elevation changes and edaphic conditions (Bertness and Ellison, 1987). Within an individual vegetative community, variability in growth habit and height was also common. *Spartina alterniflora* had three distinct variations or ecophenes observed at these sites and other marshes caused by edaphic factors: 0–50 cm (short-form [SF]); 50–100 cm (medium-form [MF]); and >100 cm (tall-form [TF]) (Anderson and Treshow, 1980; Hladik and Alber, 2012; Ornes and Kaplan, 1989; Pennings and Bertness, 2001; Reimold, Gallagher, and Thompson, 1973; Wiegert and Freeman, 1990). Tall-form typically grew along estuarine creeks with semidiurnal flooding and exceeded 2 m in height in some locations. In contrast, short-form was typically found in high marsh areas with higher salinity, sulfide concentrations, and/or lower redox potential (Mitsch and Gosselink, 2000).

Figure 3: Hatches Harbor – *Spartina alterniflora* and *Salicornia spp.* zonation along a man-made dike.

Lidar Data Collection

The National Center for Airborne Laser Mapping (NCALM) collected 37 km^2 of lidar data for this study on July 20, 2010, during peak biomass at the daily predicted low tide (± 90 minutes). The instrument used was an Optech Gemini Airborne Laser Terrain Mapper (ALTM) and an Optech 12-bit IWD-2 intelligent waveform digitizer mounted in a twin-engine Cessna 337 Skymaster (see flight parameters in Table 1). The DRL points were collected via the Optech hardware-based ranging system comprised of a constant fraction discriminator and time interval meter. Return waveforms were simultaneously digitized with a 1-ns sampling period and provided in Optech's NDF binary format with an IDX index file. The sites investigated in this research contained low growing marsh vegetation, "bare earth," and water and did not include trees, buildings, or other structures. Therefore, the data were almost entirely composed of single returns (Rogers *et al*., 2015). Elevations were initially transformed to NAVD88 using GEOID03 and later updated using GEOID09 with NOAA's Vertical Datum Transformation (VDatum) version 3.2. (NOAA NGS's latest geoid model, GEOID 12a, did not become available until after the majority of the data processing for this study was completed.)

Additionally, data were used from the lidar for the North East Project funded primarily by the American Recovery and Reinvestment Act (ARRA) of 2009 and led by the U.S. Geological Survey (USGS). These data were collected for all of Cape Cod on May 5, 2011, under senescent conditions and 9 months after the NCALM flight. The lidar data were acquired with an Optech Gemini ALTM (the same make and model of system as used by NCALM) during predicted spring low tides (± 90 minutes) at an altitude of 1,370 m AGL and a pulse rate of 145 kHz with an average point density of 3.93 pts/m^2 (Table 1). The data were collected and processed by the provider to meet a vertical accuracy of 9.25 cm (RMSE$_z$) in the "open terrain" land cover class, and elevations were referenced to NAVD88 using GEOID09.

Table 1. *Flight parameters of NCALM Jul 20, 2010, and ARRA May 5, 2011.*

Flight Parameter	NCALM	ARRA
Flying Speed (m/sec)	60	54
Altitude (m)	600	1,370
Swath Overlap (%)	50	30
Laser Beam Divergence (mrad)	0.25	0.25
Pulse Rate Frequency (kHz)	70	145
Transmit Pulse Width (ns)	12	12
Scan Rate (kHz)	40	54
Scan Angle (degrees)	± 21	± 28
Point Density (pts/m^2)	5.00	3.93
Laser Footprint Diameter (m)	0.15	0.28

Field Data Collection

A detailed set of 3,446 ground-control points (GCPs) was established in various zones that included tidal sandflats, low marshes, and high marshes. Additionally, hard surfaces such as roads and parking lots in close proximity to the marshes were surveyed to analyze overall lidar dataset accuracy. The reference data were collected with a Trimble R8 Model 3 Real Time Kinematic (RTK) GNSS rover and a Trimble NetR5 base station network with cellular-based correction. Special care was needed to ensure vertical accuracy when using the rover unit in marsh environments (Torres and Styles, 2007). A survey rod was modified with a 12-cm diameter flat base to prevent the rod from sinking into the unconsolidated mud and peat. Ground elevations were recorded in arbitrary transects through the marsh with an average point spacing of 5–7 m. The equipment manufacturer specifies the RTK GNSS enables RMSEs of < 1 cm in the horizontal and ~2 cm in the vertical (assuming ellipsoid elevations). All collected elevations were referenced to NAVD88 using GEOID09, the latest National Geodetic Survey (NGS) geoid model available at the time the airborne lidar data were provided. At most of the locations, dominant vegetation species and vegetation heights were logged for later comparisons with the lidar dataset. The field data collected with the RTK GNSS were checked to verify that accuracy standards were maintained. Comparisons were made against published benchmark elevations, as well as project control established by static GNSS using the same Trimble receiver with occupation times > 4 hours and processed with respect to Continuously Operating Reference Stations (CORS) using NGS's Online Positioning User Service (OPUS). Also, temporary benchmarks were established by occupying the same hard surface locations several times throughout the field day and computing the mean and standard deviation of the repeatedly measured elevations. Each elevation error, ΔZ, was calculated as

$$\Delta Z_i = Z_{lidar} - Z_{GPS} \quad (1)$$

The sample standard deviation (indicating the spread of the elevations about the mean) for the repeatedly surveyed temporary benchmarks was determined to be 0.006 m. The computed RMSE$_z$ was 0.006 m, calculated as follows:

$$RMSE_z = \sqrt{\frac{\sum_{i=1}^{N}(\Delta Z_i)^2}{N}} \quad (2)$$

Discrete-Return Lidar Processing

NCALM provided as part of its data deliverable a LAS file of last return lidar points and a "bare earth" grid, with point classification performed in TerraSolid TerraScan software. Upon visual inspection of the "bare earth" grid, the filtering method for ground appeared aggressive with large sections of a 14-m wide by 1.6-km long stone dike completely eliminated by the filtering. This issue may have any number of causes and is likely a result of specific parameter settings. However, because several different gridding and filtering methods were to be examined, this data deliverable was not chosen as the sole source for analysis. Discrete lidar return data from both temporal datasets were preprocessed using QPS Fledermaus 7.43 from the original LAS point cloud data. Data evaluation and cleaning were performed using the Fledermaus PFM 3D point cloud editor to remove artifacts and erroneous or non-natural points that could influence the ΔZ or gridding results. After cleaning, the point clouds were converted to raster with a grid resolution of 1 m using several different algorithms (inverse distance weighted [IDW] 1x, IDW 3x, minimum bin, maximum bin). IDW 1x used an inverse distance weighted average of only the points that fell within the 1- by 1-m cell, while the IDW 3x used a weighting of all lidar returns within a 3- by 3-m grid area surrounding the target cell. The IDW 1x method provides a better estimate of the value of each pixel based on the available lidar returns without any influence of the surrounding points, while IDW 3x method smooths the data slightly and suppresses high-frequency noise. The minimum bin and maximum bin

filtering methods use the lowest or highest value of all the lidar returns found in the grid cell and ignore all other values in the cell. Data were then imported into ESRI ArcGIS 10 for point feature and grid-based analysis using Spatial Analyst.

Lidar fundamental vertical accuracy was evaluated using hard surface control data collected with the RTK GNSS on flat surfaces such as roads and parking lots (n = 101), and the mean was then used to obtain estimates of lidar bias (Brovelli, Cannata, and Longoni, 2004; Latypov, 2002; Rosso, Ustin, and Hastings, 2006) (Figure 4). Lidar bias is defined as the mean elevation error (Rosso, Ustin, and Hastings, 2006; Sadro, Gastil-Buhl, and Melack, 2007). These surfaces should provide the best lidar return, produce minimal scatter, and will not be influenced by variable conditions such as overlying vegetation or soil moisture content. Elevation errors (ΔZ) were calculated for all hard surface points (n = 101), and the mean was then used to obtain estimates of lidar bias (Brovelli, Cannata, and Longoni, 2004; Latypov, 2002; Rosso, Ustin, and Hastings, 2006) (Figure 4). Lidar bias is defined as the mean elevation error:

$$\mu_l = \frac{\sum_{i=1}^{N} \Delta Z_i}{N} \qquad (3)$$

Due to how elevation error is defined (Equation 2), a positive bias indicates that the lidar elevations are generally above (*i.e.*, higher than) the reference elevations. In this study, it was found that the lidar underestimated the RTK GNSS elevations of hard surfaces with a bias of –0.087 m and –0.044 m for the NCALM and ARRA datasets, respectively (Table 2). Accuracies between flights were calculated from the same hard target data points to determine any global bias that may prevent an accurate assessment. The non-vegetation-induced bias was then removed to allow for unbiased comparisons between flights (Rosso, Ustin, and Hastings, 2006) and the field-collected elevations. After non-vegetation-induced bias removal, the salt marsh vegetation was analyzed in a similar manner looking at differences between lidar-derived elevation grids, surveyed ground elevations (n = 2,898), and field-collected information such as vegetation species or plant height. In this analysis, r^2, goodness-of-fit, except where noted as r, and Pearson correlation were used. All regressions and Pearson correlations reported in this paper are statistically significant with a $p < 0.05$, unless otherwise noted.

Table 2. *Hard target difference (m) between lidar measurement on pavement and RTK GNSS (n = 101) for each lidar flight.*

	NCALM	ARRA
Mean	–0.087	–0.044
Min	–0.250	–0.243
Max	0.128	0.200
StDev	0.072	0.102
$RMSE_z$	0.113	0.110

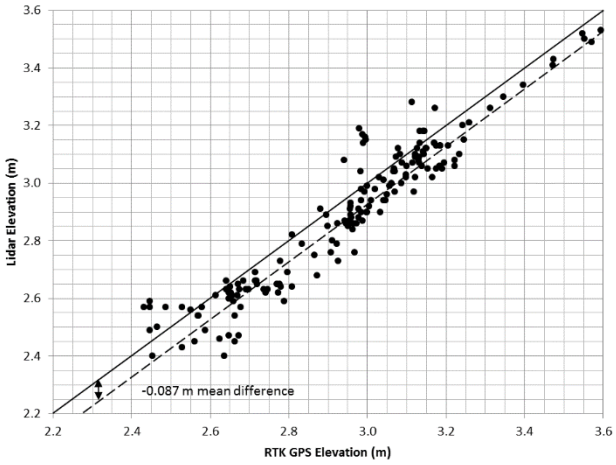

Figure 4: Scatterplot of RTK GNSS elevation against NCALM lidar elevation NAVD88 (n = 101) on hard targets (pavement). Solid line is a 1:1 correlation where the dashed best fit line has the same slope but is offset by a mean difference of –0.087 m.

Relative Uncertainty Surfaces

Lidar waveforms were extracted by developing a custom workflow using ArcGIS, QCoherent LP360, and MATLAB to compute waveform shape-related metrics. Extending previous work (Parrish, Rogers, and Calder, 2014; Rogers *et al*., 2015), the ability to create relative uncertainty surfaces (RUS) from features computed from lidar waveforms was evaluated. This process entailed first computing lidar return width for each lidar point within each marsh. The regression equations obtained from the best-fitting regressions of lidar errors (ΔZ) on waveform features developed in Parrish, Rogers, and Calder (2014) were then applied to every lidar waveform return within a subset of the project sites. The equation used was as follows with w representing waveform width (full width half maximum [FWHM]) and μ_w representing waveform mean (a measure of the center of the return pulse):

$$\widehat{\Delta Z} = \mathrm{f} \cdot \mathrm{x} \qquad (4)$$

where $\mathrm{x} = [1 \quad w \quad \mu_w \quad w \cdot \mu_w]^T$ and $\mathrm{f} = [9.0696 \quad -0.6419 \quad -0.3055 \quad 0.0207]^T$ for Moors Marsh and $\mathrm{f} = [2.3250 \quad -0.1726 \quad 0.0334 \quad -0.0029]^T$ for Pamet Marsh. The output was scaled to an arbitrary range of 0–1 (with 1 representing the highest relative uncertainty), interpolated to a regular grid (1-m grid spacing) using an inverse distance weighting (IDW) interpolation, and imported into an ArcGIS project containing imagery and other data layers for visual analysis. The reason for scaling to the arbitrary range [0 to 1] is to emphasize that the intended use of these RUS is to visually analyze spatial variation in relative uncertainty across a marsh, rather than to determine an exact value of ΔZ (with physically meaningful units, such as meters) at a particular

geographic location. The RUS grid was then lowpass filtered (using a 3x3 lowpass filter in the spatial domain) to remove high frequency noise and produce a smoother grid. This process workflow is illustrated graphically in Figure 5.

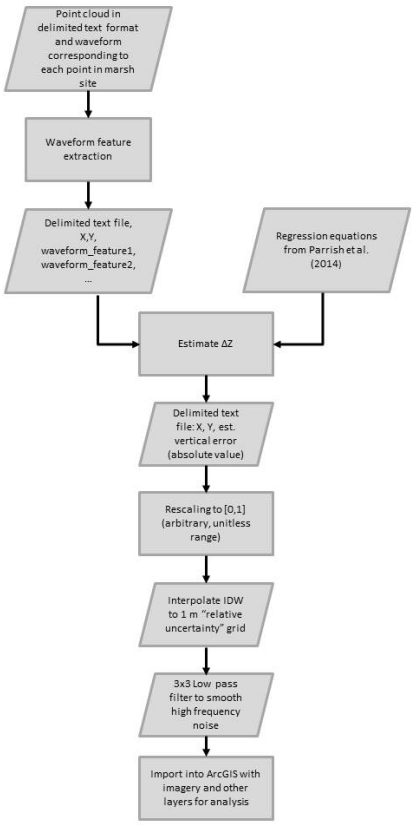

Figure 5. Workflow diagram for generation of relative uncertainty surfaces (RUS).

RESULTS

Vegetation-induced bias was investigated across all four marsh sites using a comparison of 2,648 field RTK GNSS measurements with lidar-derived elevations from the July 20, 2010, NCALM dataset. The reason for focusing primarily on bias, rather than on standard deviation and/or RMSEz, is that previous studies (Hladik and Alber, 2012; Morris *et al*., 2005; Populus *et al*., 2001; Schmid, Hadley, and Wijekoon, 2011; Torres and Styles, 2007) have shown that salt marsh vegetation introduces errors in lidar data that are generally systematic (*i.e.*, a high bias), rather than random. However, an important component of the analysis included also computing the standard deviation and RMSEz for each site and verifying that the following relationship is satisfied for large sample sizes:

$$RMSE_z^2 \approx \mu^2 + \sigma^2 \qquad (5)$$

where μ is the bias and σ is the standard deviation.

Discrete-Return Lidar Uncertainty Analysis

Several different gridding interpolation and filtering methods were assessed on the NCALM dataset for their effectiveness in producing accurate ground estimates. However, all methods evaluated in this study produced DEMs that still had significant positive bias. Using one of the most common interpolation methods, IDW, with a weight of 1 cell, it was found that the lidar measurements exhibited a positive bias of 0.14 m (σ = 0.17 m), where σ is the standard deviation, over the ground control data (Figure 6). When separated by species type, most of the overall vegetation bias could be attributed to *Spartina alterniflora* with an observed bias of 0.23 m (σ = 0.20 m) (Table 3). Using an IDW 3x (interpolation with a weight of 3x3 cells) did not produce significant differences from the IDW 1x results. The Terrascan filtered grid exhibited a modest improvement over the IDW method with a positive bias of 0.11 m (σ = 0.14 m) (Figure 7). This method also produced several points with high negative errors. A species-based review of the Terrascan

Table 3. *Difference (m) of Lidar and RTK GNSS by gridding method across all sites (all measuremetns in meters).*

Grid Method	Species	N	Mean	Min	Max	Stdev	RMS
NCALM 7/20/10 IDW1x	All Vegetation	2648	0.14	-0.34	1.12	0.17	0.22
	S. alterniflora	1390	0.23	-0.34	1.12	0.20	0.30
	S. patens	709	0.05	-0.24	0.21	0.06	0.07
	Distichlis spicata	136	0.06	-0.06	0.15	0.04	0.07
	Salicornia spp.	413	0.05	-0.13	0.33	0.06	0.08
NCALM 7/20/10 IDW3x	All Vegetation	2648	0.14	-0.22	1.13	0.17	0.22
	S. alterniflora	1390	0.22	-0.22	1.13	0.19	0.29
	S. patens	709	0.05	-0.22	0.20	0.05	0.07
	Distichlis spicata	136	0.06	-0.06	0.14	0.04	0.07
	Salicornia spp.	413	0.05	-0.13	0.30	0.06	0.08
NCALM 7/20/10 Minimum Bin	All Vegetation	2648	0.09	-0.57	1.03	0.15	0.18
	S. alterniflora	1390	0.16	-0.57	1.03	0.18	0.24
	S. patens	709	0.01	-0.28	0.19	0.06	0.06
	Distichlis spicata	136	0.02	-0.10	0.10	0.04	0.05
	Salicornia spp.	413	0.01	-0.23	0.26	0.06	0.06
NCALM 7/20/10 Terrascan Ground	All Vegetation	2648	0.11	-0.60	0.91	0.14	0.18
	S. alterniflora	1390	0.18	-0.60	0.91	0.17	0.25
	S. patens	709	0.04	-0.11	0.20	0.04	0.06
	Distichlis spicata	136	0.05	-0.07	0.12	0.04	0.06
	Salicornia spp.	413	0.04	-0.13	0.28	0.05	0.07
ARRA 5/5/11 IDW1x	All Vegetation	2648	0.04	-0.50	0.29	0.06	0.08
	S. alterniflora	1390	0.04	-0.50	0.29	0.06	0.07
	S. patens	709	0.06	-0.27	0.23	0.07	0.09
	Distichlis spicata	136	0.09	-0.03	0.17	0.04	0.10
	Salicornia spp.	413	0.01	-0.20	0.23	0.05	0.05
ARRA 5/5/11 Minimum Bin	All Vegetation	2648	0.02	-1.40	0.23	0.10	0.10
	S. alterniflora	1390	0.02	-1.12	0.23	0.08	0.08
	S. patens	709	0.02	-1.40	0.23	0.12	0.12
	Distichlis spicata	136	0.06	-1.33	0.18	0.13	0.14
	Salicornia spp.	413	-0.01	-1.07	0.21	0.10	0.10

grid was similar in its results with a majority of the overall bias attributed to *Spartina alterniflora,* which always appears to have the highest bias regardless of the processing method used.

The final methods evaluated were minimum and maximum bin filtering of the LAS data where the lowest or highest elevation reading in a defined grid cell, in this case 1 m^2, is used and all other values that occur in that grid cell are ignored. As in Schmid, Hadley and Wijekoon (2011), the minimum bin method generally improved results over the IDW method, reducing some positive data drift above the 1:1 correlation line to lower the overall bias to 0.09 m (σ = 0.15 m) (Figure 8). However, it increased the number of negative errors but decreased the standard deviation. It was initially anticipated that a) maximum bin would provide a determination of vegetation height, and b) the difference of maximum bin and minimum bin would have a correlation with bias. However, no strong relationships were found to support these assumptions.

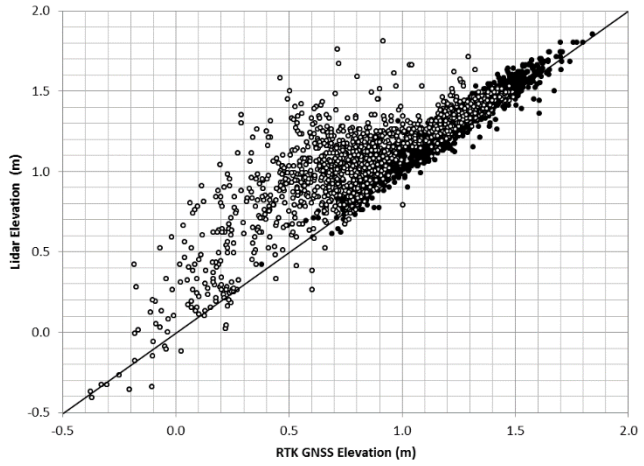

Figure 6. Scatterplot of RTK GNSS to NCALM July lidar elevations NAVD88 across all four marsh sites using the IDW 1x grid (n = 2,805). *Spartina alterniflora* is represented by an open circle and all other species are represented by a closed circle. The solid line represents 1:1 correlation.

The ARRA May 5, 2011, dataset was also evaluated with the same gridding and filtering methods, except for Terrascan, which was unavailable. This dataset represented leaf-off conditions with the marsh in its least vegetated state. As expected, this dataset was much improved over leaf-on conditions, with an overall bias of 0.04 m (σ = 0.06 m) (Figure 9). *Spartina patens* and *Distichlis spicata* were now the two species with the largest bias. Using the minimum bin approach on this dataset further reduced the overall bias but increased the standard deviation.

The results of the NCALM dataset at individual marsh sites are generally consistent with the overall lidar bias described above and are presented in Table 4. Using the IDW 1x interpolation method, the NCALM dataset had a range of bias in vegetated areas of 0.10 to 0.22 m across all sites. *Spartina patens*, *Distichlis spicata*, and *Salicornia spp*. had biases very consistent with the overall bias (*i.e*., the mean across species). However, *Spartina alterniflora* demonstrated the most variation with a site specific range from 0.16 m to 0.35 m. Results from the ARRA early season flight appear to be more varied and inconsistent at the marsh level than the peak season dataset (Table 5). There appeared to be fewer patterns of bias for individual species. At this early season flight date, *Spartina patens*, *Distichlis spicata*, and *Salicornia spp*. appear to produce larger bias than *Spartina alterniflora*.

Table 4. *Difference (m) of lidar and RTK GNSS by marsh for NCALM Flight.*

Marsh	Species		IDW - 7/20/10					Minimum Bin - 7/20/10				
		N	Mean	Min	Max	Stdev	RMS	Mean	Min	Max	Stdev	RMS
Great Island	Vegetation	532	0.11	-0.14	0.90	0.14	0.18	0.08	-0.23	0.90	0.14	0.16
	Spartina alterniflora	271	0.16	-0.06	0.90	0.18	0.24	0.13	-0.08	0.90	0.17	0.22
	Spartina patens	183	0.05	-0.06	0.17	0.04	0.07	0.02	-0.16	0.13	0.04	0.05
	Distichlis spicata	57	0.07	-0.02	0.15	0.03	0.08	0.04	-0.05	0.10	0.03	0.05
	Salicornia spp.	19	0.06	-0.05	0.21	0.06	0.09	0.03	-0.08	0.14	0.05	0.06
Hatches Harbor	Vegetation	775	0.10	-0.24	0.55	0.11	0.15	0.05	-0.51	0.52	0.10	0.12
	Spartina alterniflora	406	0.16	-0.14	0.55	0.11	0.20	0.10	-0.51	0.52	0.11	0.15
	Spartina patens	121	0.02	-0.24	0.19	0.06	0.07	-0.02	-0.27	0.19	0.07	0.07
	Distichlis spicata	57	0.07	-0.14	0.15	0.04	0.08	0.03	-0.23	0.10	0.05	0.06
	Salicornia spp.	237	0.05	-0.13	0.18	0.05	0.07	0.01	-0.23	0.16	0.06	0.06
Moors Marsh	Vegetation	819	0.22	-0.34	0.96	0.20	0.30	0.15	-0.55	0.83	0.18	0.23
	Spartina alterniflora	449	0.35	-0.34	0.96	0.18	0.39	0.26	-0.55	0.83	0.17	0.31
	Spartina patens	294	0.05	-0.17	0.21	0.06	0.08	0.01	-0.28	0.19	0.06	0.06
	Distichlis spicata	3	0.01	-0.02	0.03	0.03	0.02	-0.01	-0.03	0.01	0.02	0.02
	Salicornia spp.	56	0.05	-0.20	0.30	0.06	0.08	0.01	-0.28	0.16	0.06	0.06
Pammet Marsh	Vegetation	679	0.13	-0.23	1.12	0.19	0.23	0.06	-0.57	1.03	0.16	0.18
	Spartina alterniflora	347	0.20	-0.23	1.12	0.24	0.31	0.12	-0.57	1.03	0.21	0.24
	Spartina patens	159	0.06	-0.09	0.21	0.05	0.08	0.01	-0.25	0.18	0.07	0.07
	Distichlis spicata	65	0.05	-0.06	0.13	0.04	0.07	0.01	-0.10	0.09	0.04	0.04
	Salicornia spp.	103	0.06	-0.09	0.33	0.07	0.09	0.01	-0.13	0.26	0.07	0.07

Table 5. *Difference (m) of lidar and RTK GNSS by marsh for NCALM Flight.*

Marsh	Species		IDW - 5/5/11					Minimum Bin - 5/5/11				
		N	Mean	Min	Max	Stdev	RMS	Mean	Min	Max	Stdev	RMS
Great Island	Vegetation	532	0.09	-0.20	0.23	0.05	0.10	0.06	-1.40	0.23	0.12	0.13
	Spartina alterniflora	271	0.07	-0.06	0.23	0.05	0.09	0.05	-1.12	0.23	0.09	0.10
	Spartina patens	183	0.11	-0.16	0.21	0.04	0.12	0.08	-1.40	0.23	0.12	0.15
	Distichlis spicata	57	0.12	0.03	0.17	0.03	0.12	0.08	-1.33	0.18	0.19	0.21
	Salicornia spp.	19	0.05	-0.20	0.23	0.09	0.10	0.04	-0.33	0.21	0.11	0.12
Hatches Harbor	Vegetation	775	0.01	-0.28	0.20	0.04	0.04	-0.02	-1.25	0.21	0.11	0.11
	Spartina alterniflora	406	0.02	-0.28	0.20	0.04	0.05	-0.01	-0.87	0.21	0.09	0.09
	Spartina patens	121	-0.01	-0.23	0.11	0.05	0.05	-0.04	-1.25	0.11	0.16	0.16
	Distichlis spicata	57	0.11	-0.03	0.17	0.04	0.12	0.07	-1.33	0.18	0.20	0.21
	Salicornia spp.	237	-0.01	-0.11	0.09	0.03	0.03	-0.03	-1.07	0.07	0.11	0.12
Moors Marsh	Vegetation	819	0.02	-0.50	0.17	0.05	0.06	0.00	-1.29	0.19	0.08	0.08
	Spartina alterniflora	449	0.02	-0.50	0.17	0.05	0.06	0.00	-0.47	0.19	0.06	0.06
	Spartina patens	311	0.03	-0.27	0.14	0.06	0.06	-0.01	-1.29	0.11	0.09	0.09
	Distichlis spicata	3	0.05	0.01	0.11	0.05	0.07	0.00	-0.05	0.06	0.05	0.04
	Salicornia spp.	56	-0.01	-0.14	0.17	0.04	0.04	-0.01	-0.24	0.16	0.07	0.07
Pamet Marsh	Vegetation	679	0.08	-0.20	0.29	0.05	0.09	0.04	-0.38	0.22	0.06	0.07
	Spartina alterniflora	347	0.08	-0.18	0.29	0.05	0.09	0.04	-0.38	0.22	0.06	0.07
	Spartina patens	164	0.09	-0.20	0.23	0.05	0.10	0.05	-0.27	0.17	0.05	0.07
	Distichlis spicata	65	0.09	0.01	0.16	0.03	0.09	0.05	-0.05	0.15	0.04	0.06
	Salicornia spp.	103	0.06	-0.10	0.19	0.04	0.08	0.03	-0.21	0.12	0.04	0.05

Overall bias and standard deviation are summary statistics frequently reported to quantify the error of lidar datasets, but observing frequency of errors reveals a distribution of lidar error unique to each species surveyed (Figure 10). Three of the four target species had unimodal distributions, while one, S. alterniflora, was clearly multimodal. Due to its three distinct

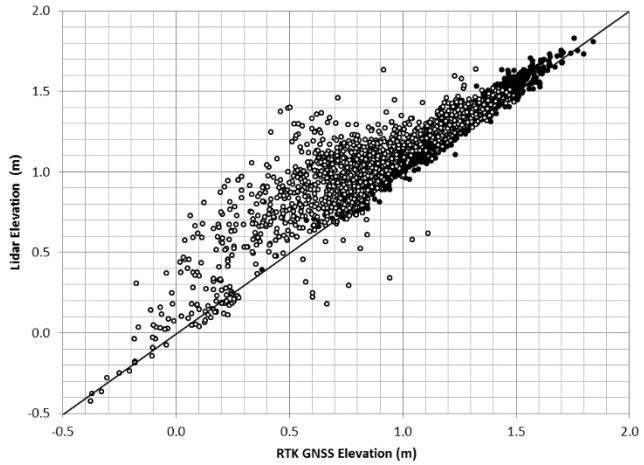

Figure 7. Scatterplot of RTK GNSS to NCALM July, Terrascan ground-filtered lidar elevations NAVD88 across all four marsh sites using the IDW 1x grid (n = 2,805). *Spartina alterniflora* is represented by an open circle and all other species are represented by a closed circle. The solid line represents 1:1 correlation.

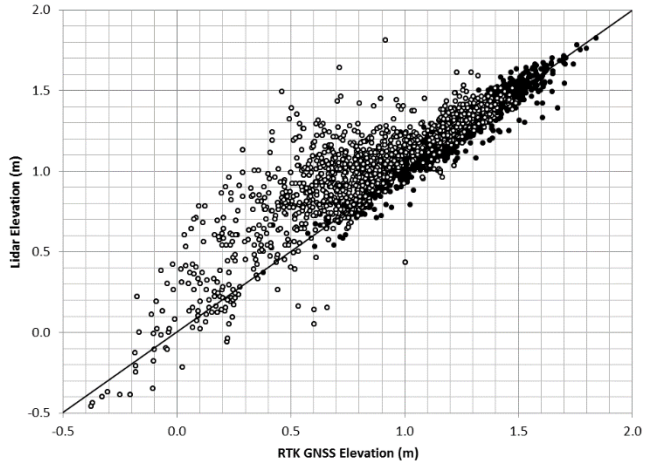

Figure 8. Scatterplot of RTK GNSS to NCALM July lidar elevations NAVD88 across all four marsh sites using the Minimum Bin grid (n = 2,805). *Spartina alterniflora* is represented by an open circle and all other species are represented by a closed circle. The solid line represents 1:1 correlation.

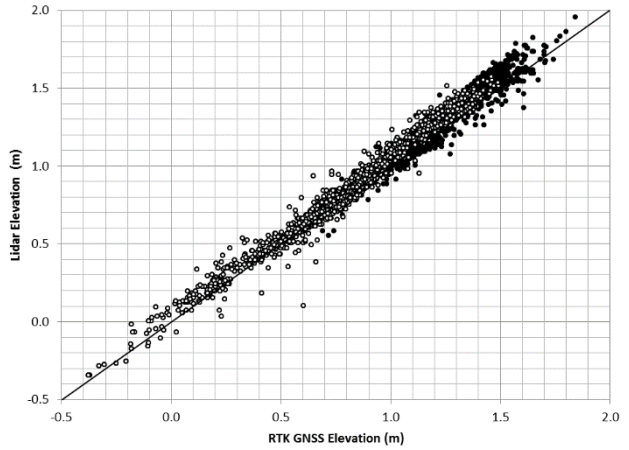

Figure 9. Scatterplot of RTK GNSS to ARRA May lidar elevations NAVD88 across all four marsh sites using the IDW 1x grid (n = 2,805). *Spartina alterniflora* is represented by an open circle and all other species are represented by a closed circle. The solid line represents 1:1 correlation.

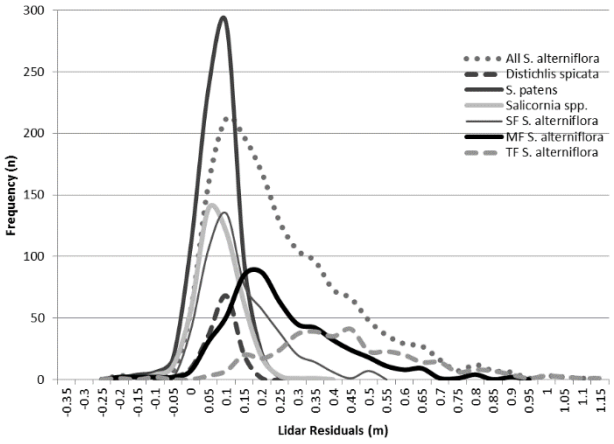

Figure 10. Frequency of occurrence for lidar errors by vegetation species using the IDW 1x grid (n = 2,805) across all four marsh sites. The thick solid line represents the combined total of all *S. alterniflora* ecophene errors [SF – Short-Form (<0.5 m), MF – Medium-Form (0.5–1 m), TF – Tall-Form (>1 m)].

ecophenes, each distribution was also plotted. The short-form *S. alterniflora* error distribution had a bias of 0.12 m (σ = 0.12 m) (n = 509). It has a similar peak as the other shorter species but with a slightly longer tail. The medium-form *S. alterniflora* exhibited a bias of 0.23 m (σ = 0.17 m) and also had an extended tail toward higher errors (n = 530). Last, the tall-form S. alterniflora showed a broad distribution with a bias of 0.41 m (σ = 0.21 m) (n = 349).

The role of vegetation height as a source of lidar bias was likewise examined. The mean height for all vegetation at 2,648 RTK GNSS locations was 0.46 m (σ = 0.38 m), with a minimum height of 0.02 m and a maximum recorded height of 1.95 m. *Spartina alterniflora* was significantly taller than the three other major species present in these marshes (Table 6). The mean height for *Spartina alterniflora* (short-, medium-, and tall-forms combined) was 0.68 m (σ = 0.38 m), with a minimum height of 0.03 m and a maximum height of 1.95 m. Lidar errors (the

difference between the NCALM IDW 1x grid and RTK GNSS elevation) plotted with the recorded vegetation heights at the same locations exhibited an $r^2 = 0.49$ (n = 2,648) (Figure 11). A regression of only the S. alterniflora locations exhibited an r^2 of 0.36 (n = 1,473). The bias to height ratio (the mean of the ratio of lidar errors to vegetation heights) was calculated for each species and represents the amount of lidar bias as a function of the vegetation height. The overall bias to height ratio was 34% for all vegetation species at the four field sites. Three of the individual species surveyed, *Spartina alterniflora*, *Spartina patens*, and *Distichlis spicata*, had a bias to height ratio of 35%, while *Salicornia spp*. was observed to have a lower ratio of 25%.

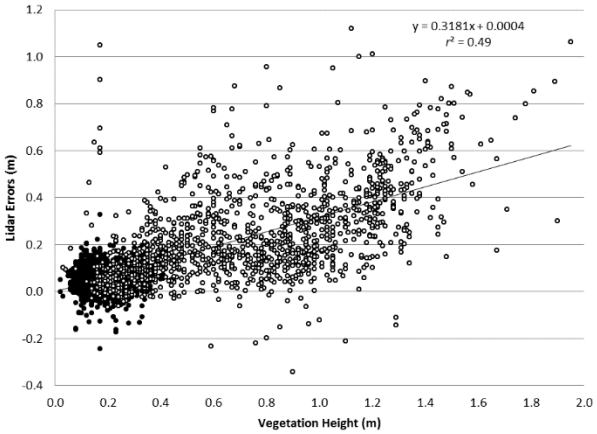

Figure 11. Scatterplot of lidar errors across all four marsh sites using the IDW 1x grid (n = 2,805) and field-measured vegetation height. *Spartina alterniflora* is represented by an open circle and all other species are represented by a closed circle. A regression of only the *Spartina alterniflora* exhibits an r^2 of 0.36 (n = 1,473).

Table 6. *Vegetation heights (cm) across all four marsh sites collected during the NCALM July 20, 2010, lidar flight. The bias to height ratio (BHR) is the mean of the ratio of lidar errors to vegetation heights.*

Analysis	N	Mean	Min	Max	SD	BHR
All Vegetation	2,648	0.46	0.02	1.95	0.383	34%
Spartina alterniflora	1,473	0.68	0.03	1.95	0.385	35%
Spartina patens	781	0.18	0.02	0.41	0.078	35%
Distichlis spicata	136	0.22	0.08	0.42	0.085	34%
Salicornia spp.	258	0.19	0.05	0.27	0.051	25%

Temporal Analysis

To look at the effects of seasonal vegetation growth on the lidar accuracy, a comparison of the May 2011 lidar data with the July 2010 dataset was conducted at the same 2,810 ground control points. It was assumed prior to data collection that the July dataset, acquired at peak vegetation conditions, would display increased elevation bias over the near-senescent early May flight. The results support this assumption, with the July dataset displaying an overall increase in bias of 0.1 m (Table 7). A graph of this comparison exhibits a strong positive bias above the 1:1 correlation line (Figure 12). When evaluated by species, GCP locations where *Spartina alterniflora* was dominant exhibited the most significant increase in elevation bias of 0.18 m. However, very little change or slight negative change was observed for the other high marsh species surveyed.

Table 7. *Difference in meters between the ARRA May 5, 2011, and the NCALM July 20, 2010, lidar flights across all four marsh sites (n = 2,648).*

Analysis	N	Mean	Min	Max	SD	RMS
All Vegetation	2,648	0.10	–0.14	1.06	0.17	0.20
Spartina alterniflora	1,390	0.18	–0.12	1.06	0.19	0.26
Spartina patens	709	–0.01	–0.11	0.20	0.05	0.05
Distichlis spicata	136	–0.03	–0.10	0.06	0.03	0.05
Salicornia spp.	413	0.04	–0.14	0.40	0.06	0.07

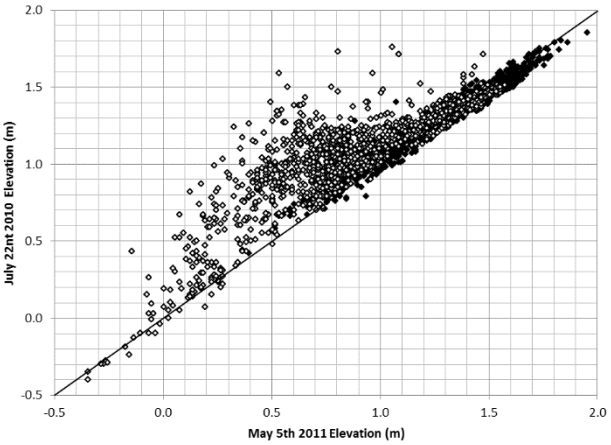

Figure 12. Plot of lidar elevation NAVD88 from the ARRA May 5, 2011, flight and the NCALM July 20, 2010, flight across all four marsh sites. The solid line represents 1:1 correlation. *Spartina alterniflora* is represented by an open circle (n = 1,473) while all other survey vegetation species are represented by a closed circle (n = 1,337).

To qualitatively and quantitatively evaluate change due to growth/seasonal variation, a difference map was created by subtracting the grid of the May flight from the July flight (Figure 13), producing a visual representation of the changes occurring across the marsh. Overall, there was a net positive increase in marsh elevations as recorded by the DRL system. Clear patterns of tall vegetation near the tidal channels and in the lowest reaches of the marsh are evident and correspond with the distribution of *Spartina alterniflora* observed during fieldwork and with aerial photography. These areas of intense change ranged up to 1 m in height in tight concentrations. Based on an analysis of 381,654 pixels of marsh surface in a subset of Moors marsh, the mean difference was 0.27 m ($\sigma = 0.19$ m) with a minimum of –0.34 m and a maximum of 1 m (Figure 14). There were very few pixels that indicated a negative change between leaf-on and leaf-off conditions within the marsh subset analyzed. The presumed underlying cause of the temporal change is the growth of the vegetation. Evaluating the grid difference with the field-measured vegetation heights exhibited a correlation with an $r^2 = 0.59$ (n = 789) (Figure 15). However, a comparison between observed discrete lidar errors (ΔZ = IDW 1x – RTK GNSS) of the NCALM 2010 flight with the difference between the ARRA May 5, 2011, and the NCALM July 20, 2010, lidar flights for the Moors marsh site had an $r^2 = 0.91$ (n = 785) (Figure 16), indicating that the errors are indeed associated with areas of taller vegetation.

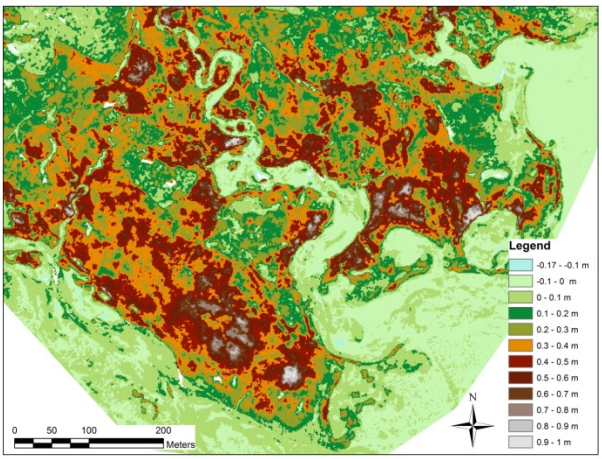

Figure 13. Difference map of increased marsh surface elevations from the ARRA May 5, 2011, and the NCALM July 20, 2010, lidar flights for Moors marsh.

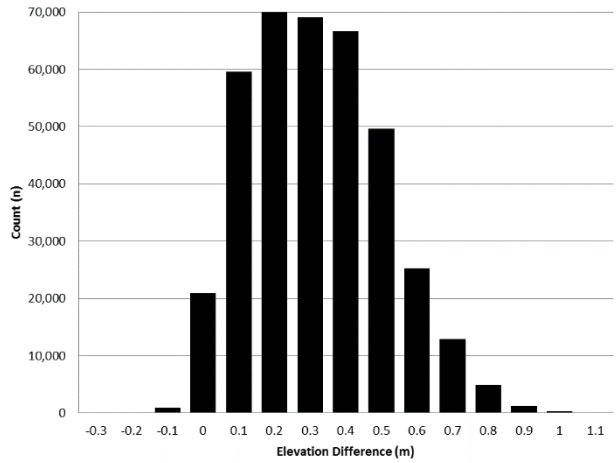

Figure 14. Histogram of marsh surface elevation differences from grids of the ARRA May 5, 2011, and the NCALM July 20, 2010, lidar flights (n = 381,654) for Moors marsh.

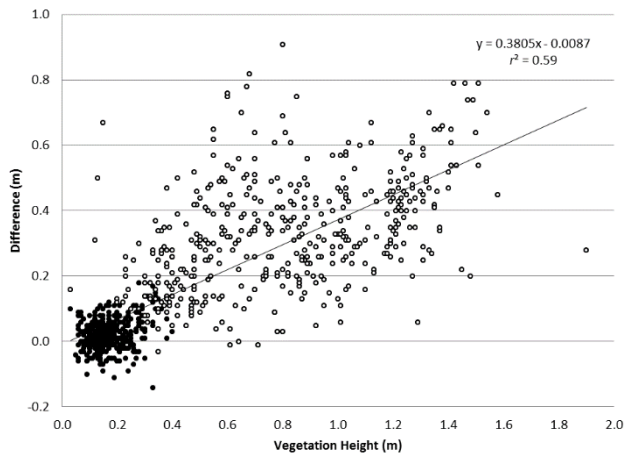

Figure 15. Relationship of the elevation difference between the ARRA May 5, 2011, and the NCALM July 20, 2010, lidar flights with field-recorded vegetation height (n = 788) across all four marsh sites. *Spartina alterniflora* is represented by an open circle (n = 436), while all other vegetation species surveyed are represented by a closed circle (n = 352).

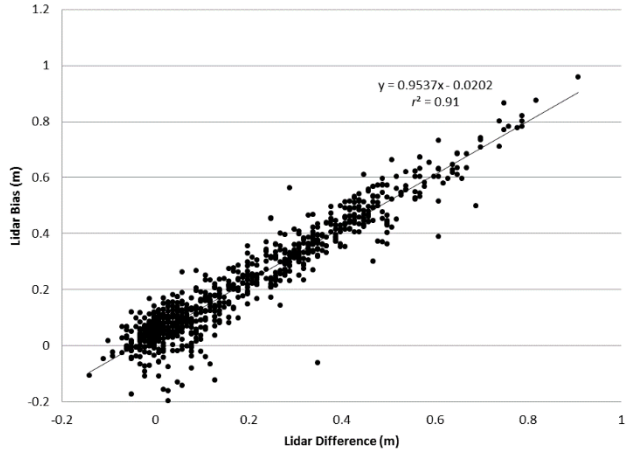

Figure 16. Relationship of discrete lidar elevation bias (ΔZ = IDW 1x – RTK GNSS) of the NCALM dataset with the difference between the ARRA May 5, 2011, and the NCALM July 20, 2010, lidar flights (n = 785) for the Moors marsh site.

Relative Uncertainty Surfaces

The next step in this study was to build upon previous work using lidar waveform feature-based metrics, waveform width and waveform mean, as they relate to both vertical uncertainty and vegetation height (Parrish, Rogers, and Calder, 2014; Rogers *et al.,* 2015). Using the regression equation above (Equation 4) from Parrish, Rogers, and Calder (2014), each individual waveform was mapped to an uncertainty value and then normalized to a relative value between 0–1 before gridding. The RUS were obtained in this manner for Moors marsh and Pamet marsh (Figure 17). Qualitatively, these maps display intricate detail as to the spatial variability in vertical error. Visual inspection of the RUS indicated that the areas of greatest uncertainty correspond with distributions of MF and TF *Spartina alterniflora*.

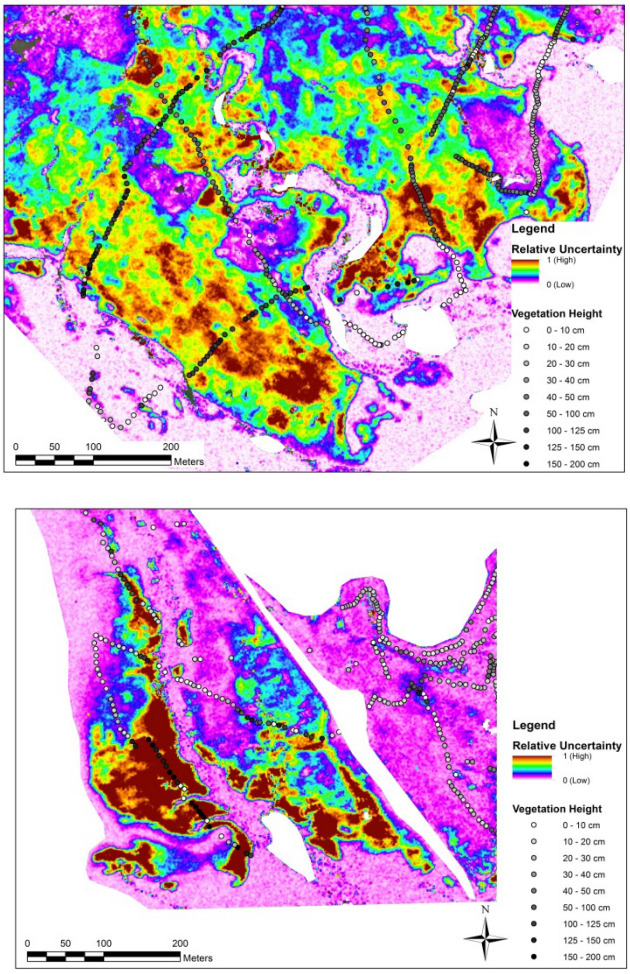

Figure 17. (a) Relative uncertainty surface (RUS) for Moors marsh developed from lidar waveform shape metrics. (b) RUS for Pamet marsh. Relative uncertainty surfaces contain unitless values scaled to the range [0–1]. This product is intended to provide a depiction of the general variation in elevation uncertainty across the marsh. Field locations are color coded by vegetation height and plotted over the RUS for general comparison.

Several quantitative analyses were conducted on these uncertainty surfaces to determine how well they represent ground conditions. The results of the RUS analysis are presented in terms of Pearson's correlation coefficient (r) since the goal was to merely determine whether there were any relationships between the variables. The first was a comparison between the waveform relative uncertainty value and the discrete-return lidar errors (ΔZ) at Pamet marsh, which exhibited a correlation of r = 0.86 (n = 271) (Figure 18). As lidar errors and vegetation height are assumed to be correlated, a comparison of the waveform uncertainty value and vegetation height was also conducted (Figure 19), which produced an r = 0.85 (n = 268). Last, the temporal analysis conducted between the July 2010 and May 2011 flights produced a detailed difference map attributable to seasonal vegetation growth. A subset of this grid sharing the same spatial extent as the waveform RUS grid was produced and the values of waveform uncertainty and temporal difference for each grid cell were compared. This procedure created a database of 380,024 values, which when plotted was extremely difficult to interpret visually due to tens of thousands of points plotting on top of one another. To refine the results to an interpretable graph, a random subset of 2,000 points was extracted (Figure 20). The overall *r* was 0.82 (n = 380,024), and four individual subsets of 2,000 randomized points had *r* values of 0.81, 0.89, 0.82, and 0.86.

DISCUSSION

Discrete Lidar Uncertainty

Comparison of DRL with RTK GNSS ground-truth elevations yielded interesting, if not unexpected, results. Overall, ground elevations were not well mapped in either the spring or fall flights by the lidar sensor within vegetated portions of the marsh. However, the spring dataset resulted in measurements closer to ground (bias of 0.04 m, σ = 0.06 m) because senescent vegetation was flattened or removed over the winter. A positive lidar bias of 0.14 m (σ = 0.17 m) was observed in the vegetated salt marsh surfaces of the July flight (Table 3). When individual vegetation species were separated, a majority of the bias can be attributed to just one species during the July flight. *Spartina alterniflora* produced a bias of 0.23 m (σ = 0.20 m), while the three other species in this study had a combined bias of approximately 0.05 m (σ = 0.06 m). The vertical growth habit of *Spartina alterniflora* is very different from the other species surveyed, which are low growing matt-like plants with mean heights less than 0.22 m (Table 6). *Spartina alterniflora* was observed to grow vertically with stalks 4–5 cm apart and 0.2–2.0 m in height with narrow, interlocking leaves near the top of the canopy. This growth form appears to greatly impact lidar pulse returns (Rogers *et al*., 2015). A regression of lidar errors and recorded vegetation heights at GCPs exhibited a significant but moderate coefficient of determination, r^2 = 0.49. The association is similar to that found by Schmid, Hadley, and Wijekoon (2011) and displayed significant scatter, suggesting high

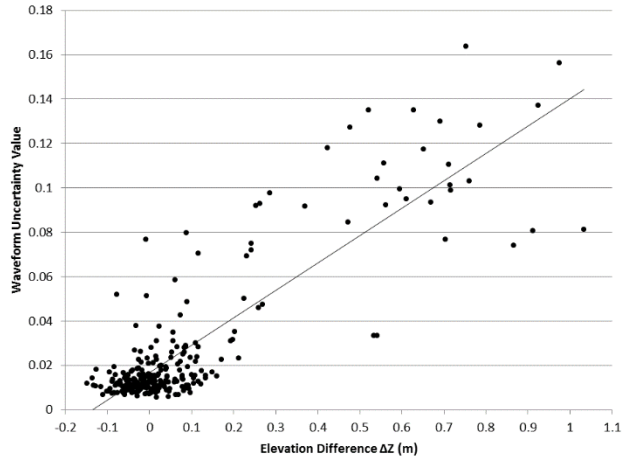

Figure 18. Relationship of the waveform relative uncertainty value with lidar bias (ΔZ) for all vegetation types (n = 271) at Pamet marsh from the NCALM July 20, 2010, dataset. The Pearson correlation coefficient (*r*) is presented.

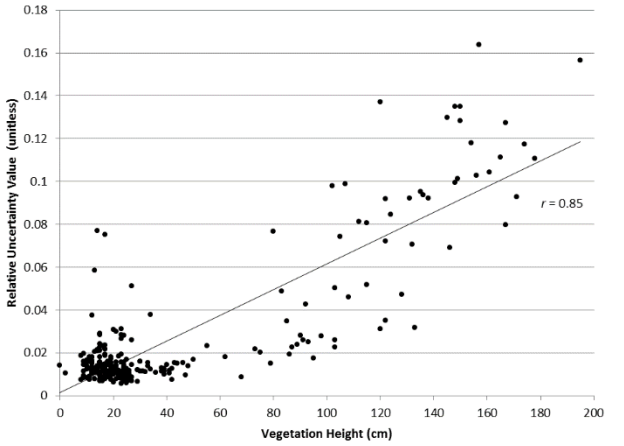

Figure 19. Relationship of the waveform relative uncertainty value with vegetation height for all vegetation types (n = 268) at Pamet marsh from the NCALM July 20, 2010, dataset. The Pearson correlation coefficient (*r*) is presented.

variability within the vegetation and the possibility of other factors influencing the increased lidar errors such as stem density, biomass density, or proportion vegetative area (PVA), a measure of the cross-sectional area and the light obscuring properties of the vegetation (Rogers *et al*., 2015).

Using various gridding and filtering methods, it may be possible to improve the overall DEM quality and lower lidar bias. For instance, using a minimum bin approach produced an improvement to overall lidar bias from 0.14 m (σ = 0.17 m) down to 0.09 m (σ = 0.17 m) when compared with the inverse distance weighting method for the July flight (Table 3). This is also consistent with findings by Schmid, Hadley, and Wijekoon (2011), but minimum bin can have certain disadvangates. For example, in the ARRA data in this study, minimum bin reduced the bias but increased the standard deviation. Additionally, in non-vegetated, open terrain areas, minimum bin often favors lowest points that are erroneous (these would normally have been ignored, filtered out, or averaged into a series of points within a grid cell). Thus, minimum bin can produce poor results in areas such as mud/sand flats or steeper slopes of tidal streams (Schmid, Hadley, and Wijekoon, 2011). There is a large difference of effectiveness of minimum bin between the shorter species and the taller *S. alterniflora* (Table 4). Maximum bin filtering did not perform as well as was initially expected. A strong correlation between the difference of maximum and minimum bin with either the field-collected vegetation height or the observed lidar errors would have been a strong case supporting the use of these methods as part of a DEM improvement strategy. Bare earth filtering algorithms such as provided in Terrascan can reduce some of the vegetation-induced elevation bias, but they are not a panacea for the challenges of lidar mapping of salt marshes and can introduce other issues/artifacts.

Intuitively, it appears that without an effective correction technique to remove lidar bias from DRL datasets, minimizing

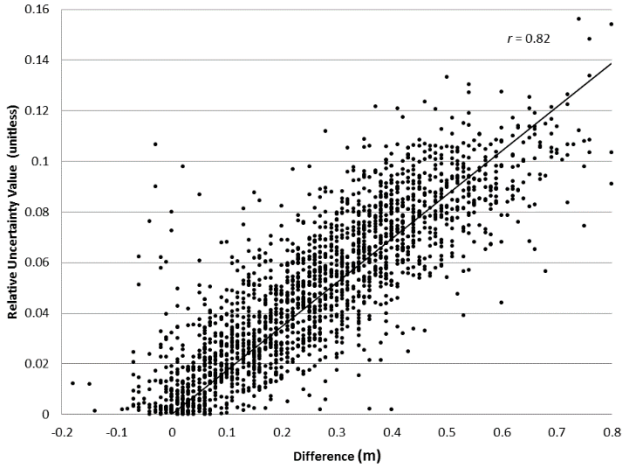

Figure 20. Relationship of the waveform relative uncertainty value with randomly selected subset of difference measurements (n = 2,000) at Moors marsh from grids of the ARRA May 5, 2011, and the NCALM July 20, 2010, lidar flights. The Pearson correlation coefficient (*r*) is presented.

bias in salt marsh environments requires that lidar flights should be coordinated during leaf-off, senescent conditions. However, senesced vegetation from the previous growing season also appears to impact the DRL pulse returns (Table 3) (Hladik and Alber, 2012; Schmid, Hadley, and Wijekoon, 2011). Winter/early spring flights during senescent conditions are not always logistically feasible, and in the case of storm assessments, coastal areas must be surveyed immediately. Furthermore, in some locations such as in the southeastern United States, the vegetation does not fully senesce. The May

dataset, as a result of the season, had an overall lidar bias of 0.04 m, which was a 0.10-m reduction over the July dataset. This reduction in bias is the direct result of the vegetation being dead and/or removed from the marsh. These findings are consistent with those of other researchers (Montane and Torres, 2006; Morris *et al*., 2005; Schmid, Hadley, and Wijekoon, 2011). Montane and Torres (2006) found senescent vegetation in South Carolina to have an overall bias of approximately 0.07 m. Another consideration when surveying colder northern climates is the impact of heavy winter snow/ice, which can be present on the marsh surface. The weight of the snow/ice sometimes compresses or strips the vegetation (*i.e.*, *Spartina alterniflora* stalks) to the ground line (Ewanchuk and Bertness, 2004). In addition, ice can even temporarily depress the marsh surface (Argow and Fitzgerald, 2006) or permanently alter marsh surface elevations by rafting vegetation/sediment (Redfield, 1972; Van Proosdij, Ollerhead, and Davidson-Arnott, 2006).

This research shows changes in DEM surfaces derived from DRL between senescent and peak-growth conditions, leading to detailed maps of growth-induced bias (Figure 13). This finding further supports DRL flight planning during senescent marsh conditions. The Moors marsh difference surface exhibited significant correlation to vegetation height and lidar errors during the July flight. It seems natural that seasonal variations in elevation detected by DRL would be related to observed lidar errors and vegetation heights. Yet even more interesting was the difference surface's strong relationship with the observed lidar errors (r^2 = 0.91) compared to the difference surface plotted vs. vegetation height (r^2 = 0.59). A correlation of lidar errors directly with vegetation height across all four marsh sites only yielded an r^2 of 0.49. Previous research has suggested that lidar bias may correspond to roughly half the canopy height of a given vegetation class (Populus *et al*., 2001) or that vegetation height alone was not enough to explain positive bias and that vegetation density also plays a role (Gopfert and Heipke, 2006). Schmid, Hadley, and Wijekoon (2011) suggested that the product of percent coverage (amount of the ground covered by vegetation) with vegetation height was a better correlation with lidar bias than strictly height. As demonstrated in this study by an overall bias to height ratio of 34%, the lidar bias appears to be less than the half of the canopy height estimate provided by other researchers, despite the data being collected during peak-growth conditions where previous researchers were working with senescent vegetation datasets. Even with a high PRF (pulse repetition frequency) of 125 kHz (Hladik and Alber, 2012) and a small footprint lidar, poor lidar penetration is achieved with potentially less than 3% of lidar returns from the ground surface likely to be recorded (Wang *et al*., 2009). The lower r^2 value found for seasonal difference to vegetation height compared with temporal difference surface's strong relationship with the observed lidar errors suggests that some other parameters such as planimetric obscuration (percent coverage) or biomass density must also influence lidar penetration and pulse return (Rogers *et al.*, 2015; Schmid, Hadley, and Wijekoon, 2011).

Relative Uncertainty Surfaces

In previous studies, simple, shape-related lidar waveform metrics were found to be predictive in estimating uncertainty and salt marsh biophysical parameters (Parrish, Rogers, and Calder, 2014; Rogers *et al*., 2015). Waveform features such as width and amplitude had significant correlations with lidar uncertainty, vegetation height, planimetric obscuration, and Proportion Vegetation Area (a ratio of the vertical obscuration [%] to the cross-sectional area of the measurement) (Rogers *et al*., 2015). In fact, waveform amplitude and waveform standard deviation accounted for nearly 75% of the variability in vegetation height (Rogers *et al*., 2015). The insights from those studies led to the creation of the RUS. As noted earlier, the motivation for describing these surfaces as "relative" and recording grid values using an arbitrary, unitless scale of 0–1, as opposed to reporting either estimated errors or standard uncertainty values in units of meters, is to avoid overstating the ability to predict elevation uncertainty from the waveform features. Research showed that the waveform features used to generate these surfaces were successful, on average, in predicting close to 60% of the total variation in DRL errors across marshes (Parrish, Rogers, and Calder, 2014). That analysis indicated that the strength of error prediction is sufficient for creating the RUS qualitative product shown in Figure 17, which provides a visual representation of the general variation of lidar uncertainty across the marsh. However, if the term "relative" were to be dropped and individual pixel values were assigned physically meaningful error units (*e.g.*, meters), there may be a tendency to misuse these data layers by placing too much faith in the exact value recorded at an individual pixel. Further research needs to be conducted using waveform feature metrics before more confidence can be given to these grids for project planning requiring highly accurate error estimates.

Attempts were made at analyzing and interpreting the RUS by comparing them to independently collected field data. The waveform uncertainty value correlated well with the discrete-return lidar bias and vegetation height. Also, the RUS displayed strong correlation with the temporal difference (ΔZ_t) between the July and May flights. The RUS surface is a strong indicator of lidar bias and can be used for qualitative analysis. Tall-form and medium-form ecophenes of *Spartina alterniflora* with vegetation height ranges of 0.5–2.0 m corresponded well to the higher values in the RUS. It appears likely that the waveform characteristics implemented in the RUS could be used to detect and map the boundary between high and low marsh environments with some degree of accuracy, since that boundary represents not only a change in vegetation species but also height. A qualitative product such as RUS can help plan projects even if exact uncertainty is not known or surface correction is not possible. For instance, identifying areas within the marsh where the elevations are the most reliable or potentially suspect could guide attention and resources to only the areas that require it. RUS might target field data collection and GNSS acquisition efforts, estimate vegetation height, or correlate with critical wildlife habitat and specific vegetation species of interest. RUS may also be used to quickly identify and monitor locations of change within the marsh since areas of higher uncertainty should be related to vegetation height, which in most cases will imply changes in inundation frequency. Increased inundation could be a result of SLR or represent areas that are subsiding due to other factors. MF and TF *S. alterniflora* have been shown to correlate well with RUS and grow at optimal elevations for that species (Morris *et al*., 2005). If areas on the high marsh platform, which

normally is populated by *S. patens*, suddenly begin to exhibit high RUS values, then further investigation would be necessary to determine the potential cause.

In previous studies, various attempts have been made to understand salt marsh lidar bias and improve the lidar-produced DEM through interpolation method, point cloud filtering, or classification (Morris *et al.*, 2005; Rosso, Ustin, and Hastings, 2006; Schmid, Hadley, and Wijekoon, 2011; Torres and Styles, 2007; Wang *et al.*, 2009). In addition, there have been several innovative approaches to DEM correction using vegetation mapping, both field and hyperspectral, and the determination and removal of constant, species-based mean correction values (Hladik and Alber, 2012; Hladik, Schalles, and Alber, 2013). However, this method, although an improvement on previous correction attempts, is ultimately limited because it assumes 1) *a priori* knowledge of species location, which is usually unavailable, woefully inaccurate, or requires additional sensors, processing, and interpretation that add to cost, time, and introduced errors; and 2) that each vegetation species requiring a DEM correction has a constant correction factor across its entire extent. As evidenced in this paper and visually presented in Figure 10, different marsh species, in particular the often spatially dominant *S. alterniflora*, have different ranges of bias that fall in a continuous distribution rather than a constant. This range of bias is presumably influenced by vegetation height, stem density, planimetric obscuration, biomass density, and growth habit (Hladik and Alber, 2012; Rogers *et al*., 2015; Schmid, Hadley, and Wijekoon, 2011). Using full-waveform lidar datasets, such as those used to create the RUS products, allows an interpretation of the uncertainty based on a spectrum of results rather than a constant. Future work will attempt to exploit the full-waveform's enhanced information and capabilities to develop new correction methods.

CONCLUSIONS

Vegetation-induced lidar uncertainty continues to be a challenge to researchers and coastal managers wanting to use lidar for fine topographic analysis in salt marshes. As in other environments, lidar uncertainty varies as a function of the terrain and vegetation cover type. The following conclusions can be drawn from this investigation:

(1) DRL returns in salt marsh environments include positive bias regardless of flight capture season. Positive lidar bias of 0.14 m (σ = 0.17 m) was observed across all survey locations in the peak vegetation dataset. A majority of the bias can be attributed to just one species, *Spartina alterniflora.*
(2) Custom interpolation and filtering techniques such as minimum bin may improve overall accuracy but can introduce additional errors, potentially creating negative bias considerations while not addressing a majority of the species-specific bias.
(3) Different marsh species have diverse ranges of bias that fall in a continuous distribution of errors rather than a constant value. While most species observed in this study have unimodal distributions, *S. alterniflora* has a multimodal distribution as a result of its three distinct ecophenes. This multimodal distribution complicates currently developed correction techniques.
(4) Temporal measurements of change in vegetation-induced-bias between peak and senescent growth conditions are possible from lidar datasets. This finding further supports DRL flight planning during senescent marsh conditions and the ability of the sensor to discriminate small vegetation-induced elevation changes.
(5) Waveform feature metrics can be used to create RUS that are useful to predict regions of variable uncertainty that can be confidently used for targeted ground truth or other field work activities.

The results of this study suggest that it may be possible to achieve at least a coarse understanding of lidar bias across an entire marsh from analysis of the lidar data alone without the a priori knowledge of vegetation species location. RUS maps can be used to minimize the amount of expensive, time-consuming field work, target specific habitats, or possibly monitor marsh change over time as it may relate to SLR and restoration initiative. Achieving this goal will require further research to extend analyses to marshes in different regions of the country with differing vegetation species and further develop a correction technique using full-waveform feature-based uncertainty surfaces to improve lidar accuracy in salt marsh environments.

ACKNOWLEDGMENTS

The authors are grateful to Dr. Nicholas C. Kraus for his support. We would like to acknowledge the following organizations and people for their contributions and funding of this research. National Center for Airborne Laser Mapping (NCALM) for providing a data grant that flew the 2010 lidar coverage for Cape Cod, Massachusetts field areas. Michael Sartori and Juan Fernandez of NCALM provided information related to the waveform acquisition. Funding for Larry G. Ward was provided by UNH/NOAA Joint Hydrographic Center Award NA10NOS4000073. Mark Adams from the Cape Cod National Seashore and Dr. Mark Borrelli from the Provincetown Center for Coastal Studies provided use of their RTK GNSS equipment for field data collection and software for data processing. We would also like to express gratitude to Dr. Mary Martin, Dr. Susan Adamowicz, and Dr. Graham Giese for their input and thoughtful reviews that helped improve this manuscript. This research was conducted as part of the requirements for completion of a doctoral degree at the University of New Hampshire Graduate School.

LITERATURE CITED

Adams, T.; Beets, P., and Parrish, C., 2012. Extracting more data from LiDAR in forested areas by analyzing waveform shape. *Remote Sensing*, 4(3), 682–702.

Anderson, C.M. and Treshow, M., 1980. A review of environmental and genetic factors that affect height in Spartina alterniflora Loisel (Salt-Marsh Cord Grass). *Estuaries*, 3(3), 168–176.

Argow, B.A. and Fitzgerald, D.M., 2006. Winter processes on northern salt marshes: evaluating the impact of in-situ peat compaction due to ice loading, Wells, ME. *Estuarine Coastal and Shelf Science*, 69(3–4), 360–369.

Bertness, M.D. and Ellison, A.M., 1987. Determinants of pattern in a New England salt marsh plant community. *Ecological Monographs*, 57(2), 129–147.

Brock, J. and Sallenger, A., 2001. *Airborne topographic LIDAR mapping for coastal and resource management. U.S. Geological Survey Open File Report 2001-46*, 4p.

Brovelli, M.; Cannata, M., and Longoni, U., 2004. LIDAR data filtering and DTM interpolation within GRASS. *Transactions in GIS*, 8(2), 155–174.

Collin, A.; Archambault, P., and Long, B., 2011. Predicting species diversity of benthic communities within turbid nearshore using full-waveform bathymetric LiDAR and machine learners. *PloS one*, 6(6), e21265.

Costanza, R.; D'arge, R.; Degroot, R.; Farber, S., and Grasso, M., 1997. The value of the world's ecosystem services and natural capital. *Nature*, 387(6630), 253–280.

Ewanchuk, P.J. and Bertness, M.D., 2004. Structure and organization of a northern New England salt marsh plant community. *Journal of Ecology*, 92(1), 72–85.

Gopfert, J. and Heipke, C., 2006. Assessment of lidar DTM in coastal vegetated areas. *International Archives of Photogrammetry, Remote Sensing, and Spatial Information Sciences*, 36(3), 79–85.

Green, J.; Carswell, D., and Gutelius, B., 1996. Topographic terrain mapping using scanning airborne laser radar. *Annual conference and exposition on GIS and LIS* (Denver, Colorado), pp. 1108–1121.

Hladik, C. and Alber, M., 2012. Accuracy assessment and correction of a LIDAR-derived salt marsh digital elevation model. *Remote Sensing of Environment*, 121(0), 224–235.

Hladik, C.; Schalles, J., and Alber, M., 2013. Salt marsh elevation and habitat mapping using hyperspectral and LIDAR data. *Remote Sensing of Environment*, 139(0), 318–330.

Hodgson, M.E. and Bresnahan, P., 2004. Accuracy of airborne lidar-derived elevation: Empirical assessment and error budget. *Photogrammetric Engineering and Remote Sensing*, 70(3), 331–339.

Hopkinson, C.; Chasmer, L.E.; Zsigovics, G.; Creed, I.F.; Sitar, M.; Treitz, P., and Maher, V., 2004. Errors in lidar ground elevation and wetland vegetation height estimates. *International Archives of Photogrammetry, Remote Sensing, and Spatial Information Sciences*, 36(8), 108–113.

Jutzi, B. and Stilla, U., 2006. Range determination with waveform recording laser systems using a Wiener Filter. *ISPRS Journal of Photogrammetry and Remote Sensing*, 61(2), 95–107.

Latypov, D., 2002. Estimating relative lidar accuracy information from overlapping flight lines. *ISPRS Journal of Photogrammetry and Remote Sensing*, 56(4), 236–245.

Lefsky, M.A.; Cohen, W.B.; Parker, G.G., and Harding, D.J., 2002. Lidar remote sensing for ecosystem studies. *BioScience*, 52(1), 19–30.

Mallet, C. and Bretar, F., 2009. Full-waveform topographic lidar: State-of-the-art. *ISPRS Journal of Photogrammetry and Remote Sensing*, 64(1), 1–16.

Mitsch, W.J. and Gosselink, J.G., 2000. *Wetlands*. New Jersey: Wiley & Sons, 582p.

Montane, J.M. and Torres, R., 2006. Accuracy assessment of lidar saltmarsh topographic data using RTK GPS. *Photogrammetric Engineering and Remote Sensing*, 72(8), 961–967.

Morris, J.T.; Porter, D.; Neet, M.; Noble, P.; Schmidt, L.; Lapine, L.A., and Jensen, J.R., 2005. Integrating Lidar elevation data, multispectral imagery and neural network modeling for marsh characterization. *International Journal of Remote Sensing*, 26(23), 5221–5234.

Morris, J.T.; Sundareshwar, P.V.; Nietch, C.T.; Kjerfve, B., and Cahoon, D.R., 2002. Responses of coastal wetlands to rising sea level. *Ecology*, 83(10), 2869–2877.

Muss, J.D.; Aguilar-Amuchastegui, N.; Mladenoff, D.J., and Henebry, G.M., 2013. Analysis of waveform lidar data using shape-based metrics. *IEEE Geoscience and Remote Sensing Letters*, 10(1), 106–110.

Nayegandhi A.; Brock, J.C.; Wright, C.W., and O'Connell, M.J., 2006. Evaluating a small footprint, waveform-resolving lidar over coastal vegetation communities. *Photogrammetric Engineering & Remote Sensing*, 72(12),1407–1417.

NOAA, 2013. *Tides and Currents*. http://tidesandcurrents.noaa.gov/inventory.html?id=8446121.

Ornes, W.H. and Kaplan, D.I., 1989. Macronutrient status of tall and short forms of Spartina alterniflora in a South Carolina salt marsh. *Marine Ecology-Progress Series*, 55(1), 63–72.

Parrish, C.E.; Rogers, J.N., and Calder, B.R., 2014. Assessment of waveform features for lidar uncertainty modeling in a coastal salt marsh environment. *IEEE Geoscience and Remote Sensing Letters*, 11(2), 569–573.

Pennings, S.C. and Bertness, M.D., 2001. Salt Marsh Communities. *In*: Bertness, M.D., Gaines, S.D., and Hay, M.E. (eds.), *Marine Community Ecology*. Sunderland, MA: Sinauer Associates Inc., pp. 289–316.

Populus, J.; Barreau, G.; Faxilleau, J.; Kerdreux, M., and L'yavanc, J., 2001. Assessment of the Lidar topographic technique over a coastal area. *Proceedings of CoastGIS'01: 4th International Symposium on GIS and Computer Mapping for Coastal Zone Management* (Halifax, Nova Scotia), 11p.

Portnoy, J.W.; Roman, C.T.; Smith, S.M., and Gwilliam, E., 2003. Estuarine habitat restoration at Cape Cod National Seashore: the Hatches Harbor prototype. *Park Science*, 22(1), 8.

Redfield, A.C., 1972. Development of a New England salt marsh. *Ecological Monographs*, 42(2), 201–237.

Reimold, R.J.; Gallagher, J.L., and Thompson, D.E., 1973. Remote sensing of tidal marsh. *Photogrammetric Engineering and Remote Sensing*, 39(5), 477–488.

Rogers, J.N.; Parrish, C.E.; Ward, L.G., and Burdick, D.M., 2015. Evaluation of field-measured vertical obscuration and full waveform lidar to assess salt marsh vegetation biophysical parameters. *Remote Sensing of Environment*, 156(0), 264–275.

Rosso, P.H.; Ustin, S.L., and Hastings, A., 2006. Use of lidar to study changes associated with Spartina invasion in San Francisco Bay marshes. *Remote Sensing of Environment*, 100(3), 295–306.

Sadro, S.; Gastil-Buhl, M., and Melack, J., 2007. Characterizing patterns of plant distribution in a southern California salt marsh using remotely sensed topographic and hyperspectral data and local tidal fluctuations. *Remote Sensing of*

Environment, 110(2), 226–239.
Schmid, K.A.; Hadley, B.C., and Wijekoon, N., 2011. Vertical accuracy and use of topographic LIDAR data in coastal marshes. *Journal of Coastal Research*, 27(6A), 116–132.
Shrestha, R. and Carter, W.E., 1998. Engineering applications of airborne scanning lasers: Reports from the field. *Photogrammetry Engineering and Remote Sensing*, 64(4), 256.
Smith, S.M., 2009. Multi-decadal changes in salt marshes of Cape Cod, MA: photographic analyses of vegetation loss, species shifts, and geomorphic change. *Northeastern Naturalist*, 16(2), 183–208.
Tiner, R.W.J., 1987. *A Field Guide to Coastal Wetland Plants of the Northeastern United States*. Amherst: University of Massachusetts Press, 285p.
Torres, R. and Styles, R., 2007. Effects of topographic structure on salt marsh currents. *Journal of Geophysical Research-Earth Surface*, 112(F2), 14.
Van Proosdij, D.; Ollerhead, J., and Davidson-Arnott, R.G.D., 2006. Seasonal and annual variations in the volumetric sediment balance of a macro-tidal salt marsh. *Marine Geology*, 225(1–4), 103–127.
Wang, C.; Menenti, M.; Stoll, M.P.; Feola, A.; Belluco, E., and Marani, M., 2009. Separation of ground and low vegetation signatures in LiDAR measurements of salt-marsh environments. *IEEE Transactions on Geoscience and Remote Sensing*, 47(7), 2014–2023.
Wiegert, R.G. and Freeman, B.J., 1990. *Tidal salt marshes of the southeast Atlantic Coast: a community profile*. Washington, D.C.: U.S. Dept. of the Interior, Fish and Wildlife Service, 70p.